

Abstract Booklet



University of Cambridge

8th -9th January 2025

Our sponsors



AIXTRON



Invited Talk:

Carrier transport and recombination in wide InGaN quantum wells

Prof Dr. Ulrich Schwarz

Technical University Chemnitz, Germany

Thin quantum wells (QWs) enabled blue LEDs by increasing carrier density and electron-hole wave-function overlap, thus boosting internal quantum efficiency (IQE). This is common wisdom, and almost all LEDs and laser diodes in the short visible spectrum are based on few nanometers thin InGaN QWs. Recently it was demonstrated, that InGaN quantum wells with thickness beyond 10 nm can result in LED with high IQE or laser diodes with large differential gain, if the piezoelectric field can be screened. These InGaN QWs with wide QWs were grown by plasma-assisted molecular beam epitaxy (PAMBE). They enable new device concepts and deliver interesting insights in carrier transport and recombination in wide wells. I will discuss three topics: First, the transition from quantum-well to bulk-like behavior with increasing screening of thick InGaN QWs. The dynamics of this transition is observed when the emitter is driven with short current pulses. Secondly, enhanced lateral carrier diffusion due to the long carrier lifetime. Thirdly, the observation of radiative recombination from hot carriers. The latter two observations are possible because of the extremely long carrier lifetime of the dark states in un-screened wide quantum well.

Invited Talk:

Multiscale simulation of recombination processes and carrier transport in III-N heterostructures

Dr Stefan Schulz

Tyndall National Institute and University College Cork, Ireland

Semiconductor heterostructures utilizing III-N alloys have attracted considerable research interest due to their potential for optoelectronic device applications. However, and in comparison to other III-V semiconductor heterostructures, wurtzite III-N-based systems exhibit very different fundamental properties. This starts with the underlying crystal structure, ranges over to the presence of very strong electrostatic built-in fields and ultimately the observation of carrier localization effects in III-N alloys. In this talk, the impact of (random) alloy fluctuations on charge carrier transport, radiative and non-radiative recombination processes in wurtzite III-N heterostructures will be discussed.

Contributed Abstracts:

The FeGa(0/-) acceptor defect level in dilute Al_xGa_{1-x}N

Dr Piotr Kruszewski¹, Dr Jerzy Plesiewicz¹, Dr Sz Grzanka¹, Dr E. Grzanka¹, Dr P. Prystawko¹, Dr Vladimior Markevich², Prof. Anthony Peaker², Mr. Lijie Sun², Mr Christopher Dawe², Dr Iris Liu³, Prof. Jim Speck³, Prof. David Binks², Prof. Matthew Halsall²

¹Institute of High Pressure Physics, ²University of Manchester, ³The University of California Santa Barbara

Defects that generate energy levels deep within the bandgap play a pivotal role in influencing the performance of GaN/AlGaN devices. Despite their critical impact, the understanding of many of these deep-level defects remains limited [1]. This limitation primarily stems from the challenge of deciphering the intricate interplay among various types of defects and impurities present in typical GaN/AlGaN structures.

In this work, we study defects with deep levels both in high-quality dilute Al_xGa_{1-x}N ($x \leq 0.063$) samples grown by metal-organic vapor phase epitaxy (MOVPE) on highly conductive native Ammono-GaN substrates and also in GaN samples grown by molecular beam epitaxy (MBE) on different sapphire substrates. These samples have been characterized by using a combination of deep-level transient spectroscopy (DLTS), high-resolution Laplace DLTS (L-DLTS) and low-temperature photoluminescence (PL) spectroscopy.

L-DLTS and PL have been used to demonstrate that the FeGa (0/-) acceptor level in dilute Al_xGa_{1-x}N ($x \leq 0.063$) can be considered as a common reference level, as expected for energy levels of transition metals in isovalent semiconductor compounds (Fig.1). Furthermore, the conduction and valence band offsets (ΔE_c and ΔE_v , respectively) in GaN/Al_xGa_{1-x}N heterojunctions have been found as a function of Al content for samples grown by the metalorganic vapor-phase epitaxy technique on native Ammono-GaN substrates. The band-offsets determined in this study are $\Delta E_c = 1.17x$ eV and $\Delta E_v = -0.95x$ eV over the range of x studied and are in good agreement with other experimental results reported for actual GaN/Al_xGa_{1-x}N heterojunctions as well as with the recent theoretical calculations based on hybrid density functional theory (Fig.2) [2]. Meanwhile, we also report significant Fe defect related peaks existing on MBE-GaN samples from both DLTS and PL (Fig.3), confirming that iron can be found in a range of GaN materials.

Deep level traps in as-grown epilayers of (010) β -Ga₂O₃ grown by metal organic chemical vapour deposition on native Sn-doped substrates

Mr Christopher Dawe¹, Dr Vladimir Markevich¹, Professor Matthew Halsall¹, Dr Ian Hawkins¹, Dr Janet Jacobs¹, Prof Anthony Peaker¹, Mr Arpit Nandi², Dr Indraneel Sanyal², Prof Martin Kuball²

¹University Of Manchester, ²University of Bristol

β -Ga₂O₃ has significant potential in power electronics due to its large breakdown fields, high Baliga figure of merit and the ability to grow high-quality epilayers on large-area native substrates [1]. Performance of some β -Ga₂O₃-based electronic and optoelectronic devices are influenced by defects with deep energy levels in the bandgap. Therefore, several studies of deep-level defects in β -Ga₂O₃-based materials and devices have been reported [2]. However, a comprehensive understanding of deep-level defects in β -Ga₂O₃ is still missing. An effective method for elucidating the properties of electrically active defects in β -Ga₂O₃ is deep-level transient spectroscopy (DLTS) in conjunction with Laplace-DLTS (L-DLTS) [3].

DLTS and L-DLTS have been used to characterise deep-level traps in as-grown (010) β -Ga₂O₃ epilayers grown by MOCVD on native Sn-doped substrates. Two types of epilayers have been studied, one doped with silicon to $\sim 1.5 \times 10^{17} \text{ cm}^{-3}$, the other was unintentionally doped (UID). Four electron traps with emission activation energies (ΔE_c) of 0.10, 0.42, 0.53 and 0.66 eV have been detected in both epilayers, with the Si-doped epilayer exhibiting larger trap concentrations (N_T) for each level. Our findings support suggestions that the E0.10 trap is related to Si_Ga(II) [4]. Dependence of electron emission rate (e_{em}) on the electric field (E) for the E0.10 trap is characteristic of a donor level, while that for the E0.42 trap indicates an acceptor level. The concentration-depth profiles $\{N_T(W)\}$ show non-uniform spatial distributions for both the E0.10 and E0.42 traps in the UID samples, indicating out-diffusion from the substrate/interface into the epilayer as a likely source.

References

- [1] A. J. Green et al. APL Mater 2022, 10, 029201.
- [2] A. Langørgen et al. J. Appl. Phys. 2024, 135, 195702
- [3] A. R. Peaker et al. J. Appl. Phys. 2018, 123, 161559.
- [4] A. T. Neal et al. Sci Rep, 2017, 7, 13218

Thermal assessment of AlGaN alloys using ns-thermoreflectance

Mr Leo Norman¹, Zeina Abdallah, James Pomeroy, Gergana Drandova, Jose Jimenez, Andy Xie, Antonio Lucero, Martin Kuball

¹CDTR University of Bristol

Aluminium Gallium Nitride (AlGaN) is a promising material in modern electronics and optoelectronics [1], particularly valued for its tuneable wide bandgap and its role in the formation of the 2DEG in GaN transistors [2]. These qualities make AlGaN ideal for high-power and high-frequency devices, including ultraviolet (UV) LEDs [3] and high-electron-mobility transistors (HEMTs). However, as AlGaN's composition varies, so does its thermal conductivity (κ), affecting device performance and reliability. Studying the compositional dependence of AlGaN κ at different temperatures is crucial to assess its impact on device thermal performance.

Nano-second time-domain thermoreflectance (ns-TDTR), which is an optical pump-probe method [4], was used to investigate the κ of AlGaN with different Al composition, from 0 to 6%, at different temperatures. Figure (a) shows the temperature dependent κ of pure GaN and AlGaN with 1-6% Al composition. This demonstrates that the addition of just 1% Al can dramatically impact the κ due to alloy-phonon scattering. For example, at 25°C, the κ decreases from 145 W/mK for pure GaN to 38 W/mK for 1% AlGaN. Furthermore, the temperature dependency of the κ also changes due to impact of scattering phenomena. Further alloying of AlGaN affects the κ , but the temperature dependence is found to be similar to that of 1% AlGaN.

These measurements are essential for verifying semi-empirical models, such as the Callaway model [5], often used to predict lattice thermal conductivities in semiconductors. While these models assess phonon contributions only, they can fall short due to underestimation of scattering processes [6] and varied growth methods. Figure (b) presents the Callaway model (dashed lines) along with the ns-TDTR measured thermal conductivities (symbols) at 25°C. It shows that the Callaway model overestimates the κ , and therefore highlights the need for experimental results to accurately study the effect of integrating AlGaN into device design.

References:

- [1] Mishra, U.K., Parikh, P. and Yi-Feng Wu (2002). AlGaN/GaN HEMTs-an overview of device operation and applications. *Proceedings of the IEEE*, [online] 90(6), pp.1022–1031. doi:<https://doi.org/10.1109/jproc.2002.1021567>.
- [2] Koley, G. and Spencer, M.G. (2005). On the origin of the two-dimensional electron gas at the AlGaIn/GaN heterostructure interface. *Applied Physics Letters*, 86(4), p.042107. doi:<https://doi.org/10.1063/1.1850600>.
- [3] Hasegawa, H., Maeda, N., Fujikawa, S., Toyoda, S. and Kamata, N. (2014). Recent progress and future prospects of AlGaIn-based high-efficiency deep-ultraviolet light-emitting diodes. *Japanese Journal of Applied Physics*, 53(10), pp.100209–100209. doi:<https://doi.org/10.7567/jjap.53.100209>.
- [4] Garrelts, R., Marconnet, A. and Xu, X. (2015). Assessment of Thermal Properties via Nanosecond Thermoreflectance Method. *Nanoscale and Microscale Thermophysical Engineering*, 19(4), pp.245–257. doi:<https://doi.org/10.1080/15567265.2015.1078425>.
- [5] Callaway, J. (1959). Model for Lattice Thermal Conductivity at Low Temperatures. *Physical Review*, 113(4), pp.1046–1051. doi:<https://doi.org/10.1103/physrev.113.1046>.
- [6] Ma, J., Li, W. and Luo, X. (2014). Examining the Callaway model for lattice thermal conductivity. *Physical Review B*, 90(3). doi:<https://doi.org/10.1103/physrevb.90.035203>.

Investigation of (mis-)orientation in zincblende GaN grown on micro-patterned Si(001) using electron backscatter diffraction

Dale M. Waters¹, Bethany Thompson¹, Gergely Ferenczi¹, Ben Hourahine¹, Grzegorz Cios², Aimo Winkelmann^{1,2}, Christoph J. M. Stark³, Christian Wetzel³, Carol Trager-Cowan¹, Dr Jochen Bruckbauer¹

¹University Of Strathclyde, ²AGH University of Krakow, ³Rensselaer Polytechnic Institute

Here we use the technique of electron backscatter diffraction (EBSD) for characterising wurtzite (wz) and zincblende (zb) polytypes of GaN grown on micropatterned Si (001) substrates. The Si substrate is etched to create parallel V-shaped grooves with opposing {111} facets before the deposition of GaN. EBSD reveals that wz-GaN growth fronts initially form on the {111} Si facets before undergoing a transition from a wurtzite to zincblende structure as the two growth fronts meet. Orientation analysis of the GaN structures shows that the wz-GaN growth fronts have different growth orientations but share the same crystallographic relationship with the zb-GaN; such that the lowest index alignments are: $\perp\{30\text{-}38\}_{\text{wz}} \parallel \langle 110 \rangle_{\text{zb}}$, $\langle 11\text{-}20 \rangle_{\text{wz}} \parallel \langle 110 \rangle_{\text{zb}}$, and $\perp\{30\text{-}34\}_{\text{wz}} \parallel \langle 001 \rangle_{\text{zb}}$. Furthermore, the crystallographic relationship, $\{0001\}_{\text{wz-GaN}} \parallel \{111\}_{\text{zb-GaN}} \parallel \{111\}_{\text{Si}}$, and alignment of the wz- and zb-GaN with respect to the Si substrate was investigated. The two wz-GaN $\langle 0001 \rangle$ growth directions were expected to coalesce at an angle of 109.5° , however measurements revealed an angle of 108° . The resultant misalignment of $\approx 1.5^\circ$ induces misorientation in the zb-GaN crystal lattice. While the degree of misorientation within the zb-GaN lattice is low, $< 1^\circ$, the zb-GaN lattice is deformed and bends towards the wz-GaN interfaces about the specimen direction parallel to the length of the V-groove. Further EBSD measurements over larger areas of the sample revealed that these results were consistent across the sample. However, it was also observed that there are additional changes in the orientation of the zb-GaN lattice, which may relate to the initial growth conditions of the zb-GaN.

Experimental investigation of GaN transistors' radiated switching noise for low power loads

Dr Vlad Marsic¹, Dr Soroush Farammehr¹, Ms Isha Maini², Prof David Moran², Prof Petar Igic¹

¹Centre Of E-mobility And Clean Growth, Coventry University, ²School of Engineering, University of Glasgow, R526 Level 5, Eng -Micro & Nanotechnology, Rankine Building

Wide bandgap Gallium Nitride (GaN) technology promises to deliver the next generation of power transistors however, the electromagnetic (EM) radiofrequency (RF) emissions due to GaN power switching require extra design resources while their mechanism is not well understood and documented.

In this work through practical experimentation the GaN transistor's EM RF switching noise was monitored and mapped for two different devices from the same brand at variable loads and functioning frequencies. The two main observations regarding GaN transistor's switching noise resulted from this study were published in 2024 together with other electromagnetic investigations in [1] and, they are succinctly described as follows:

- for GaN transistors the RF emissions are only on the switching OFF time, resulting that accelerated electrons on the Larmor formula will emit only when braking.
- it was discovered that the EM RF switching noise is proportional to the transistor's current transfer area while its magnitude is due to electrical current required by the load.

The final assertion of this work was a straightforward explanation for all electrical switching radiated noise, which is caused by the conducted current's accelerated charges passing through a spatial area, whose size may reduce the noise if it is increased accordingly.

These findings contribute to the overall research effort for reducing power losses and EM RF noise produced by the electrical switches when designing for EM compatibility (EMC) and implicitly are delivering a high positive impact on its new family member, the GaN power transistor technology.

References:

[1] Marsic, V., Farammehr, S., Fleming, J., Bhagat, R. and Igic, P., "GaN transistors' radiated switching noise source evidenced by Hall sensor experiments towards integration", IEEE Access, pgs. 13783 – 13794, 2024, DOI: 10.1109/ACCESS.2024.3357239.

Effects of TEGa flow rate on the phase-purity of κ -Ga₂O₃ films on AlGa_N substrates in MOCVD

Khai Ngo¹, Matthew Smith¹, Martin Kuball¹

¹University of Bristol

Amongst polymorphs of Ga₂O₃, the orthorhombic κ -phase is unique for its high polarisation coefficient which permits 2D-electron gas (2DEG) formation when integrating with other ferroelectrics such as the Al_xGa_{1-x}N material system. Simulations predict 2DEG sheet carrier density up to $10^{13} - 10^{14} \text{ cm}^{-2}$ for κ -Ga₂O₃/Al_xGa_{1-x}N and 2D-hole gas (2DHG) for doped κ -Ga₂O₃/AlN structures [1, 2]. To achieve high 2DEG density experimentally, it is critical to obtain phase-pure κ -Ga₂O₃ films. While the temperature range 450 – 500°C was found to be optimal for growing κ -Ga₂O₃ on AlN by MOCVD [3], the effects of precursor flow rates on the phase-purity of κ -Ga₂O₃ grown on AlGa_N has not been systematically investigated.

Here, κ -phase Ga₂O₃ with a FWHM of 0.67° was successfully grown on 600 nm Al₇₅Ga₂₅N on sapphire templates (with 1000 nm AlN buffer layer) using Agnitron Agilis 100 MOCVD reactor. This is the best reported FWHM to date for growth by MOCVD on Al_xGa_{1-x}N templates. In addition, our results demonstrate that both the κ -Ga₂O₃ phase fraction and FWHM improve towards lower supersaturation conditions.

The temperature, pressure, and oxygen flow rate was maintained at 500°C, 10 Torr, and 80 sccm, respectively. The TEGa flow rate was varied between 200, 250, and 300 sccm. XRD 2θ - ω scans of Ga₂O₃ films on Al₇₅Ga₂₅N (Fig. 1) show that the resulting epilayers are mixed κ - and β -Ga₂O₃. Peaks in the {002} κ -Ga₂O₃ family are observed at $2\theta = 19.1^\circ$, 38.8° , and 59.85° , with shoulder peaks at $2\theta = 38.3^\circ$, and 59.1° due to {-201} β -Ga₂O₃ reflections. The volume phase fraction of κ -Ga₂O₃ $V_\kappa/(V_\kappa + V_\beta)$ was quantified based on the relative peak intensities I_κ of (006) κ -Ga₂O₃ and I_β of (-603) β -Ga₂O₃ [4]. We found that the film achieves highest κ -Ga₂O₃ phase fraction of 95% and FWHM of 0.67° for lower TEGa flow rates (Fig. 2). The trend is opposite for sapphire growth where phase-pure κ -Ga₂O₃ is favoured at high supersaturation conditions [5]. This could be due to the different strain conditions imposed on the Ga₂O₃ epilayer, which is compressive for sapphire growth but tensile for Al₇₅Ga₂₅N growth. These findings provide guidance on the optimisation of MOCVD conditions to achieve high quality κ -Ga₂O₃ films on Al_xGa_{1-x}N templates toward realization of 2-dimensional electron/hole gases at the heterointerface and subsequent fabrication of transistors.

References

- [1] Leone et al, Journal of Crystal Growth, 534, 125511 (2016)
- [2] Polyakov et al, Journal of Alloys and Compounds, 936, 168315 (2023)
- [3] Hu et al, Materials Science in Semiconductor Processing, 178, 108453 (2024)
- [4] Usman et al, Optical Materials, 145, 114373 (2023)
- [5] Bosi et al, Crystal Growth & Design, 21, 6393-6401 (2021)

Acknowledgement

We thank Rachel Oliver (University of Cambridge) for providing the Al₇₅Ga₂₅N/AlN/sapphire template, and Yidi Yin (University of Bristol) for help with cleaving the wafers.

Aluminum-Nitride-on-Sapphire Photonic Integrated Circuits Operating in the Telecommunications C-band.

Mr Davey Davis Armstrong¹, Dr Joseph Cannon¹, Ms Olivia Kiely¹, Mr Husieyn Yagci¹, Prof Anthony Bennett¹

¹Cardiff University

AlN-on-sapphire is a promising material system for the development of integrated photonic circuits operating across the ultraviolet, visible and infrared spectral ranges owing to its ultra-wide bandgap. Furthermore, piezoelectric, opto-electronic and non-linear optical coefficients enable novel components on an epitaxial platform compatible with InGaN lasers, LEDs and high-power electronics.

We have developed a set of designs for vertical grating couplers, waveguides, resonators and directional couplers which have been fabricated on commercially sourced 600 nm-thick AlN on sapphire. Using electron-beam lithography, dry etch techniques and cladding with silica we have manufactured ring resonators with smooth >85 degree vertical sidewalls. Typical all-pass resonators have intrinsic quality factors over 300,000 in the telecommunication spectrum. During the presentation we will discuss what limits the optical loss in these samples and thus the future scope for photon pair generation by spontaneous four-wave mixing in ultra-high quality factor resonators.

Nucleation layer studies of MOVPE-grown zincblende GaN

Martin Frentrop¹, Menno J Kappers¹, David J. Wallis², Rachel A. Oliver¹

¹University of Cambridge, ²Cardiff University

Cubic zincblende GaN (zb-GaN) provides a possible route to future efficient green wavelength LEDs. This is primarily motivated by the absence of polarization fields in the (001) orientation, and its lower bandgap compared to hexagonal wurtzite (wz)-GaN. However, zb-GaN films often exhibit mixed phases and a high density of {111}-type stacking faults, both of which may negatively influence the optical and electrical properties of the material. Therefore, understanding the mechanisms which lead to the formation of these defects plays a crucial role in their successful suppression and thus in achieving the high efficiencies predicted for zb-GaN based devices.

Our recent experiments show that the V/III-ratio and temperature during the initial nucleation stage of epitaxy have a profound effect on the defect structure and orientation in the subsequently grown cubic GaN thin films and that cubic GaN thin films with high phase purity can be achieved within a growth window of sufficient size for practical applications. At V/III-ratios below the optimum, the temperature window for good quality cubic GaN growth is rather narrow as wz-GaN inclusions tend to form on Ga-polar {111} polar facets. With increasing V/III ratio, wurtzite inclusions and SFs with Ga-polar character are suppressed more and more efficiently and the temperature window for cubic growth increases in size and reaches a width of up to ca. 80°C. However, above the optimum V/III-ratio SFs and wurtzite inclusions start to form with N-polar character and strong anisotropy on {1-11} facets in this temperature window, providing an upper limit for the parameter range within which cubic GaN with high phase purity can be achieved.

This knowledge of the defect formation mechanisms further allows us to engineer the distribution of SF defects and their annihilation with increasing film thickness in the subsequent cubic GaN thin films, and hence achieve low defective material.

Towards Commercial Grade Gallium Oxide Epitaxy on Large Diameter Substrates

Dr Indraneel Sanyal¹, Mr. Salwan Omar², Dr. Ken Tao¹, Dr. Andrew Pakes¹

¹Aixtron Ltd, ²Aixtron Inc

The increasing interest in gallium oxide (Ga₂O₃) research is fueled by its potential for next-generation power electronic devices designed for multi-kilovolt applications. Metalorganic Chemical Vapour Deposition (MOCVD) is the leading epitaxial growth method, offering significant advantages over other techniques by enabling controlled doping, impurity management, and the growth of alloys and heterostructures. Additionally, large native Ga₂O₃ substrates, up to 4 inches in diameter, are already commercially available, with projections for 6-inch substrates by 2026. The cost of these large Ga₂O₃ substrates is gradually decreasing, creating strong competition with the industry-standard SiC substrates. Consequently, developing Ga₂O₃ epitaxy on similarly large substrates that can be easily transferred to native substrates for commercial-grade Ga₂O₃ epitaxy is of great interest. However, significant challenges remain in achieving high-purity Ga₂O₃ layers with ultra-low background carrier concentrations, high growth rates, and good uniformity on large-diameter substrates. To date, Ga₂O₃ epitaxy on sapphire substrates up to 2 inches in diameter has been reported in the literature.

Phase-pure β -Ga₂O₃ layers grown on sapphire exhibited an XRD (-201) FWHM of 0.79° for a $1\text{ }\mu\text{m}$ thick layer. The highest quality layer was achieved on an 8° miscut substrate, showing an FWHM as low as 0.35° , by controlling the gas-phase pre-reaction through dynamic process gap adjustment. This adjustment reduces the working distance between the gas injection showerhead surface and the substrate in real-time during growth. Precise control of parasitic gas-phase reactions by dynamically adjusting the gap during growth is crucial and offers greater flexibility for optimizing growth parameters. Ga₂O₃ grown on 4-inch sapphire substrates demonstrated thickness uniformities with a standard deviation (σ) of 1% across a wide range of growth rates and reactor conditions. Additionally, wafer-to-wafer thickness variations of only 0.56% were achieved in a 3x2-inch configuration.

SIMS analysis of layers grown under suitable conditions using TMGa indicated a C level of $3.7\text{E}16\text{ cm}^{-3}$ and H concentration of $1.3\text{E}16\text{ cm}^{-3}$, both close to the SIMS detection limits. Background Si levels in the undoped layer were $4\text{E}15\text{ cm}^{-3}$, resulting in ultra-low background carrier concentration of $2\text{E}15\text{ cm}^{-3}$ as determined by Hg-probe CV measurements. Furthermore, using N₂ as a carrier gas showed no detectable nitrogen incorporation over those grown with Ar for a wide range of growth temperatures up to 1090°C .

Further results of MOCVD growth of gallium oxide on both sapphire and native Ga₂O₃ substrates will be discussed.

Indium segregation at stacking faults in zincblende InGaN epilayers

Petr Vacek¹, Martin Frentrup¹, Menno Kappers¹, David Wallis^{1,2}, Rachel Oliver¹

¹Department of Materials Science and Metallurgy, University of Cambridge, ²Centre for High Frequency Engineering, Cardiff University

Zincblende (zb) GaN epilayers grown on zb-SiC templates exhibit stacking faults and wurtzite inclusions as the predominant crystal defects. In the case of zb-InGaN, Indium (In) tends to segregate in the vicinity of defects [1], leading to significant inhomogeneities in the alloy distribution. This significantly impacts the optical and structural properties of the layer. In order to understand the In segregation in zb-InGaN epitaxial layers, we investigated the dependence of In segregation near stacking faults on the in-plane crystal orientation using scanning transmission electron microscopy (STEM).

Indium segregation near stacking faults was previously reported for InGaN quantum wells in the zone perpendicular to the miscut [1]. We observe a similar behaviour in 40 nm-thick InGaN epilayers, which show a clear segregation of In adjacent to, rather than directly on, stacking faults and wurtzite inclusions. However, the In segregation behaves differently for the orientation where the zone axis is parallel to the miscut. There, In tends to segregate directly on the stacking faults and wurtzite inclusions. This behaviour was observed using high-resolution STEM imaging and further confirmed by energy-dispersive x-ray spectroscopy (EDX) mapping.

We suggest that the difference in the In segregation near stacking faults for the two in-plane orientations is due to a different Ga- or N-polar bonding configuration at the surface step terminating a stacking fault during the epilayer growth. Alternatively, the presence of small {111}-like facets on the growth surface may affect the In incorporation for the orientation perpendicular to the miscut, while these facets may not be present for the orientation parallel to the miscut.

[1] B. Ding, M. Frentrup, S.M. Fairclough, M.J. Kappers, M. Jain, A. Kovács, D.J. Wallis, R.A. Oliver, Alloy segregation at stacking faults in zincblende GaN heterostructures, J Appl Phys 128 (2020) 145703. <https://doi.org/10.1063/5.0015157>.

Strain and luminescence properties of hexagonal hillocks in N-polar GaN

Dr Jochen Bruckbauer¹, Grzegorz Cios², Andrei Sarua³, Peng Feng⁴, Tao Wang⁵, Ben Hourahine¹,
Aimo Winkelmann^{1,2}, Carol Trager-Cowan¹, Robert W. Martin¹

¹University Of Strathclyde, ²AGH University of Krakow, ³University of Bristol, ⁴University of Sheffield,
⁵Cardiff University

Owing to its unique properties, N-polar or (000-1)-orientated GaN offers several advantages over Ga-polar or (0001) GaN for applications in high power electronics. The most significant being for high electron mobility transistors: enhanced carrier confinement of the 2-dimensional electron gas and improved device scalability. However, the growth of high-quality N-polar material is challenging. One issue that dominates is the increased surface roughness, due to the occurrence of hexagonal-shaped hillocks (or hexagons) on the material's surface. Although, there are different methods to reduce the density of these hillocks, such as the use of vicinal substrates and the use of optimal growth conditions, their properties have not been extensively studied. Here, we investigate the crystallographic and luminescence properties of these hexagonal features using the techniques of electron backscatter diffraction (EBSD) and cathodoluminescence (CL) hyperspectral imaging in the scanning electron microscope, combined with micro-Raman mapping. CL revealed increased light emission from the top of the hexagons when compared with the surrounding material. Additionally, black spots in the intensity images, associated with non-radiative recombination at threading dislocations, could be resolved on the hexagons. These are not resolvable in the surrounding area, implying increased material quality of the hexagons. Extensive strain analysis using EBSD revealed that the hexagons are under tensile strain, predominantly parallel to the m-plane sides. As the hexagons become larger from the centre to the edge, this strain increases in the radial direction. This was confirmed by mapping the Raman E2 (high) mode. Overall this provides crucial information on the strain state of these hexagonal features for improving material quality.

A cascade model for the defect-mediated electrochemical etching of porous gallium nitride distributed Bragg reflectors

Mr Ben Thornley¹, Mr Maruf Sarkar¹, Dr Saptarsi Ghosh², Dr Menno Kappers¹, Professor Rachel Oliver¹

¹Department of Materials Science and Metallurgy, University Of Cambridge, 27 Charles Babbage Road, CB3 0FS, ²Department of Electrical and Electronic Engineering, Swansea University, Bay Campus, SA1 8EN

Porous GaN distributed Bragg reflectors (DBRs) represent a novel technology for high reflectance mirrors in the nitride epitaxial system, exploiting the much higher refractive index contrast that can be achieved using porous materials compared to the conventional alloying approach. A conductivity-selective electrochemical etching (ECE) process is used to create porosity in doped layers within a stack of alternating doped/undoped layers, leaving the undoped layers notionally non-porous, achieving competitive reflectances.

ECE is performed by submerging the sample and a platinum counter electrode into an electrolyte solution and applying voltage across them. Here we study an approach in which the doped layers in the stack are porosified without the need for lithographic processing. This is achieved using the threading dislocations that pervade through the stack which act as etchant channels, opening into nano-pipes to allow etchant access. Here, for the first time, we use volumetric FIB-SEM tomography to uncover the complex interactions of the different fields of porosity emanating from different dislocations as etching proceeds through the stack, and formulate a new 'cascade' model for the interaction and activation/deactivation sequence of the different dislocations.

Three porous GaN DBRs were prepared by ECE from the same wafer (see figure 1a). ECE was performed on each sample at 5, 8 and 10 V. Tomographic FIB-SEM datasets were generated using a Zeiss Crossbeam 540 and the Atlas Nanotomography package. Segmentation of the tomograph frames allows for the precise tracking of porosity through the stack, based on which we will introduce novel "confetti diagrams" that enable large-scale calculation of dislocation statistics. This work forms the base of a new model for the porosification process, its evolution with time, and the dependence on the specifics of this process on the applied voltage, all of which will be discussed with respect to the optimisation of reflectance.

Radiation resilient (Al_xGa_{1-x})₂O₃ photodetectors for applications in Low Earth Orbit

Sean Douglas¹, Arpit Nandi², Sai Vanjara², Dr Matthew Smith², Professor Martin Kuball², Viesturs Spulis¹, Professor Robert Martin¹, Professor Paul Mckenna¹, Dr Robbie Wilson¹, Dr Ross Gray¹, Dr Stephen Reynolds³, Dr Fabien Massabuau¹

¹University of Strathclyde, ²University of Bristol, ³University of Dundee

Radiation resilient deep ultraviolet (UVC) solar-blind photodetectors are critically important to enable further technologies within the space sector, for sensing distant galaxies, stars and comets or for space communication. Therefore, it is key to demonstrate and understand the effects of radiation on the material properties.

This work aims to characterise (Al_xGa_{1-x})₂O₃ samples with a range of Al contents and demonstrate tuneable peak responsivity ranging within the 225-250nm spectral range and the radiation resilience for applications in Space.

(Al_xGa_{1-x})₂O₃ Photodetectors were fabricated by MOCVD with target Al contents of 0%, 25%, and 50%. These were then characterised for composition, surface morphology, luminescence and photoconduction properties before and after being exposed to proton and electron irradiation with energies of ~1.2 MeV using a laser plasma accelerator to simulate a four-month mission to Low Earth Orbit.

The results obtained demonstrate the radiation resilience of (Al_xGa_{1-x})₂O₃ samples with 0%, 25% and 45% Al content. Although it appears from scanning electron microscopy (SEM) imaging that possible pitting occurs only on the pure Ga₂O₃ sample when exposed to radiation. Post radiation exposure luminescence suggest greater intensity of 2.4 eV and 3.0 eV peaks suggesting an increase in vacancy defects. Photoconduction responsivity and constant photocurrent method (CPM) measurements were utilised to observe the absorption coefficient sub-bandgap and suggest a slight broadening of the band-edge which may be attributed to higher defect density.

Post radiation characteristics demonstrate the radiation resilience of (Al_xGa_{1-x})₂O₃ with little damage to surface morphology, an increase of defect states most likely Ga vacancies which are suggested by luminescence studies and a slight broadening of the absorption edge from photoconduction analysis.

Polarisation-resolved cathodoluminescence study of a zincblende InGaN/GaN single quantum well

Mr Xiuyuan Xu¹, Dr M. Frentrop¹, Dr G. Kusch¹, Dr Z. S. Pehlivan¹, Dr M. J. Kappers¹, Prof D. J. Wallis^{1,2}, Prof R. A. Oliver¹

¹Department of Materials Science and Metallurgy, University Of Cambridge, ²Centre for High Frequency Engineering, University of Cardiff

Zincblende (zb) GaN LEDs have the potential to overcome the low efficiency of long-wavelength emission because (001) zb GaN is free of internal polarization fields and has a narrower bandgap compared to wurtzite GaN [1]. However, it suffers from a high density of stacking faults (SFs), which impacts the luminescence from quantum wells (QWs). Recently, optical characteristics typical of quantum wires (QWires) were identified in zb InGaN QW cathodoluminescence (CL), attributed to indium enrichment at the intersection of SFs with a single quantum well (SQW) [2]. Meanwhile, previous photoluminescence studies suggested that the QW emission is polarised and may relate to such SF-related QWires [3].

In this presentation, we will report on polarisation-resolved CL measurements of zb InGaN/GaN SQW samples grown on zb GaN buffers with thicknesses varying from 600 nm to 3000 nm by metal-organic vapour phase epitaxy. X-ray diffraction analysis has previously shown that the SF density reduces with buffer thickness and hence a reduction in polarisation might be expected [4]. The mean spectra of panchromatic CL maps show that light emission is mainly from the QW and is highly polarised. Polarisation-resolved panchromatic CL maps show that the polarised light arises from both SFs and defect-free regions, but that the majority of the polarised emission is from defect-free regions and appears QW-like. QWire-like characteristics were observed at SF locations, supporting the suggestion QWires can generate polarised light. The degree of polarisation (DoP) was determined to be about 0.625 for the SQW emission peak in the mean spectrum and is approximately independent of SF density. If the polarised emission were largely related to QWires at SFs, the reduction in SF density with buffer thickness would lead to a lower DoP at larger thicknesses. Hence, this provides further evidence that most polarised emission is attributable to defect-free material.

Structure Evolution of Porous GaN with Defect Mediated Etching

Mr Jiawei Zhang¹, Mr Ben Thornley¹, Dr Sidra Dar¹, Dr Thom Harris-Lee¹, Dr Menno Kappers¹, Prof Rachel Oliver¹

¹University Of Cambridge

Porous GaN distributed Bragg reflectors (DBRs) obtained from electrochemical etching (ECE) were previously studied intensively and a defect-mediated etching mechanism has been reported[1]. However, in structures where (unlike in DBRs) the doping extends throughout the layer targeted for etching and up to the surface, defect-mediated etching has not usually been expected.

Here, thick (1 μm) Si-doped GaN ($n = 1.8 \times 10^{18} \text{ cm}^{-3}$) layers were porosified via ECE at a range of applied biases (6-40 V) using 0.25 M oxalic acid and characterised using atomic force microscopy (AFM), scanning electron microscopy (SEM) (Figure 1(a-c)) and focused ion beam (FIB) SEM tomography (Figure 1(d)).

The back-scattered electron (BSE) SEM images of sample surfaces (etched at 10, 24, and 32 V respectively) and SEM images of the cross-sections show evidence of successful porosification. However, at low voltages, the AFM images show a surface similar to an unetched sample. The surface pit density (Figure 2) is approximately equal to the threading dislocation density (TDD) for this material while the applied bias is low (6-20 V). This indicates that ECE is occurring via defects. Increasing the etching voltage to higher values (22-30 V) causes pits to form randomly over the sample surface until an upper limit is reached (at 30 V).

For a sample etched at low voltage (10 or 12 V, Figure 1(a, d)) significant lateral branching from vertical pores is observed, consistent with the morphologies seen in defect-mediated DBR etching[2]. At 24 V, where pits are created across the surface, pores radially branch out from these pits until depths approximately 200 nm into the doped layer. Then these pores propagate down vertically (Figure 1 (b)). When a higher voltage (32 V) is applied, more pits are observed scattered across the sample surface and the pores propagate vertically, relatively parallel to each other.

Reference:

1. Sarkar, M. et al. Microscopy and Microanalysis 30, 208–225 (2024).
2. Ghosh, S. et al. J Appl Phys 136, (2024).

Simultaneous Data Display and Environment Sensing with a MicroLED Display

Johnathan Gray¹, Jonathan J D McKendry¹, Robert K Henderson², Michael J Strain¹, Martin D Dawson¹, Johannes Herrnsdorf¹

¹University of Strathclyde, ²University of Edinburgh

Simultaneously depth-sensing and transmitting information wirelessly has become widespread in consumer technologies, from mobile devices to motion-sensing games consoles [1,2]. These features rely on separate systems, using various regions of the EM spectrum, and are independent of the display technology. ‘Megaprojector’ is a high-resolution Gallium Nitride MicroLED display capable of broad illumination across the visible spectrum [3]. A 128 × 128 array of 30 µm GaN-on-CMOS pixels allows fast pattern display up to 0.5 Mfps and simultaneous nanosecond pixel pulsing up to 100 MHz, realising display technology capable of Gbps data display and simultaneous depth sensing [3,4]. To demonstrate data transfer and depth sensing capability, pseudo-random binary patterns unique to each MicroLED were displayed at 40 kfps using a 16 x 128 subsection of the array. A conventional high-speed camera imaged the display, determining the received data per MicroLED. Simultaneously, the MicroLEDs were pulsed with a 5 ns electrical signal. A white paper target was placed in front of the display at several distances, and a single-photon avalanche diode (SPAD) detected back-scattered photons, (Fig. 1). Photon arrival times relative to the 5 ns driving pulse were collected, producing a histogram of time-of-flight (ToF) from LED to detector. Movement of the target resulted in changes to the histogram peak location, cross-correlation allowed sub-cm depth measurement. Images of the MicroLED patterns allowed comparison between transmitted and received bit-sequences at >80 Mbps with an acceptable bit-error-rate (BER) for most pixels, demonstrating high speed wireless data transfer and simultaneous sub-cm depth measurements. Sensitivity of the high-speed camera limited the display frame rate, however 333 kfps is achievable providing 5.5 Gbps. Upgrading to an array of SPADs will provide 3D imaging of the environment. Megaprojector can be used as a high-resolution MicroLED display simultaneously performing gesture recognition, but also as a communications terminal capable of sensing movement in its environment.

REFERENCES

- [1] H. Barnouti, S. S. M. Al-Dabbagh, and W. E. Matti, “Face recognition: A literature review,” *Int. J. Appl. Inf. Syst.* 11, 21–31 (2016).
- [2] Z. Zhang, “Microsoft kinect sensor and its effect,” *IEEE MultiMedia* 19, 4–10 (2012).
- [3] N. Bani Hassan, F. Dehkhoda, E. Xie, J. Herrnsdorf, M. J. Strain, R. Henderson, & M. D. Dawson (2022). Ultrahigh frame rate digital light projector using chip-scale LED-on-CMOS technology. *Photonics Research*, 10(10), 2434. <https://doi.org/10.1364/PRJ.455574>.
- [4] J. A. Gray, J. J. D. McKendry, J. H. Herrnsdorff, M. J. Strain, R. K. Henderson and M. D. Dawson, “Micro-LED Nanosecond Pulsed Structured Light Sources with 405 nm – 510 nm Wavelength,” 2023 IEEE Photonics Conference (IPC), Orlando, FL, USA, 2023, pp. 1-2, doi: 10.1109/IPC57732.2023.10360550.
- [5] A. D. Griffiths, H. Chen, D. D.-U. Li, R. K. Henderson, J. Herrnsdorf, M. D. Dawson, and M. J. Strain, “Multispectral time-of-flight imaging using light-emitting diodes,” *Opt. Express* 27, 35485 (2019).

Multimodal micro-spectroscopy for quantifying compositional and phase variations in $(\text{In}_x\text{Ga}_{1-x})_2\text{O}_3$ thin films

Dr Naresh Gunasekar³, Dr Daniel Hunter¹, Mr Raed Alshammary³, Dr Paul Edwards¹, Prof. Holger Wenckstern², Prof. Marius Grundmann², Prof. Robert Martin¹

¹Department of Physics SUPA University of Strathclyde Glasgow G4 0NG, UK, ²Felix-Bloch-Institut für Festkörperphysik, Fakultät für Physik und Geowissenschaften, Universität Leipzig, Linnestraße 5, 04103 Leipzig, Germany, ³Institute for Compound Semiconductors, School of Physics and Astronomy, Cardiff University, Cardiff CF24 3AA, UK

Crystalline indium gallium oxide $(\text{In}_x\text{Ga}_{1-x})_2\text{O}_3$ alloys are generating immense research interest for applications in next-generation optical and electronic devices, particularly photodetectors¹, solar cells², and high-electron mobility transistors³. The possibility of tailoring the bandgap from $\sim 3 - 5$ eV, the ability to control the surface space charge, and improvement in the large-area deposition techniques offer exciting opportunities for this alloy system. However, the different thermodynamically stable crystal structures of In_2O_3 (cubic) and Ga_2O_3 (monoclinic) cause bandgap miscibility and phase separation. This work is motivated by the need for a detailed investigation of the physical properties of this alloy system throughout the whole composition range to support the design of newer compound semiconductor devices.

Pulsed laser deposition was used to grow $(\text{In}_x\text{Ga}_{1-x})_2\text{O}_3$ on sapphire in the composition range of $(0.01 < x < 0.82)$ across the 50 mm wafer ⁴. We have applied wavelength dispersive X-ray spectroscopy (WDX) for compositional analysis, optical transmission spectroscopy and cathodoluminescence spectroscopy (CL) to study optical properties together with electron backscatter diffraction (EBSD) and Raman spectroscopy to understand the structural properties. Fig 1a shows the WDX mapping of In across the 2-inch wafer, revealing In and Ga-rich regions. Fig 1b shows the Raman spectra acquired from specific locations where phase segregation is observed and verified using EBSD. We were able to elucidate the specific Raman modes that are present in the cubic phase (3mm), mixed phase (9mm) and monoclinic phase (44mm). We compared the light emission properties via CL spectroscopy from these areas, showing the deterioration of the crystal quality when the In composition is increased, evident from the increase in the FWHM of the emission peak corresponding to the recombination of free electrons and self-trapped holes and also from the loss in the EBSD pattern quality. Our work highlights the specific Raman modes, CL peaks, and crystal planes that can be assessed to rapidly quantify wafers of $(\text{In}_x\text{Ga}_{1-x})_2\text{O}_3$ alloys.

References:

1. Isa Hatipoglu et al J. Phys. D: Appl. Phys. 53, 454001(2020)
2. Jamarkattel et al ACS Appl. Energy Mater. 5, 5484 (2022)
3. Mazzolini et al ACS Appl. Mater. Interfaces 16, 12793 (2024)
4. Swallow et al ACS Appl. Mater. Interfaces 13, 2807 (2021)

4 kV β -Ga₂O₃ trench Schottky barrier diodes: reliability, defects and failure mechanisms

Dr. Sai Charan Vanjari^{1,2}, Mr. Aditya Bhat Kundapura¹, Ms. Haiqi Huang¹, Dr. James Pomeroy¹, Dr. Matthew Smith¹, Prof. Martin Kuball^{1,2}

¹University Of Bristol, ²Innovation and Knowledge Centre REWIRE

High-voltage power electronics rely on kV-class semiconductor devices for efficient power switching. Beta-gallium oxide (β -Ga₂O₃), with its ultra-wide band gap of 4.8 eV and a large breakdown field of 8 MV/cm, has emerged as a promising alternative to commercially available wide band gap technologies for high-voltage applications. Advancements in melt growth methods, such as edge-defined film-fed growth (EFG) [1], Czochralski (CZ) [2], and vertical Bridgman (VB) [3], have enabled the commercialization of cost-effective 4-inch Ga₂O₃ wafers, while larger 6-inch wafers are expected to be available soon, further expanding its market potential. Despite these advancements, several challenges persist in the commercialization of Ga₂O₃ devices such as vertical Schottky barrier diodes, with conventional planar structures being limited by poor electric field management and the absence of p-doping compounds the challenges in harnessing the true potential of the material. Unipolar devices architectures such as the trench Schottky barrier diodes have shown promise in achieving high breakdown voltages [4], but further device-level innovations are crucial to optimize the electric field control and boost the overall performance further. In addition, the role of crystallographic defects in influencing high-voltage reliability remains an area requiring deeper investigation. In this work, we present our latest advancements in demonstrating state-of-the-art 4 kV Ga₂O₃ trench Schottky barrier diodes (TSBDs). High-voltage reliability testing was conducted up to 3 kV using a step stress method, revealing minimal degradation in on-resistance ($R_{on,sp}$), with only a 13% increase after prolonged stress durations. The potential trapping mechanisms at dielectric/semiconductor interface were studied using TCAD simulations. Post-breakdown analysis revealed that these devices often exhibited failure cracks along the [010] crystallographic direction in Ga₂O₃ wafers with (001) orientation. These cracks aligned with the orientation of platelike nanopipe defects, a type of crystallographic defect originating from the melt-grown substrates. To assess whether these defects contribute to electrical breakdown, we performed defect and failure-site mapping using laser confocal microscopy and scanning electron microscopy. Our findings indicate that platelike nanopipe defects are not the primary cause of failure for the majority of the devices investigated. Instead, the failure-induced cracks are predominantly attributed to the weak crystallographic (100) planes in Ga₂O₃, as confirmed by nanoindentation measurements.

References

- [1] H. Aida, et al. Japanese Journal of Applied Physics, 47(11R), 8506, 2008.
- [2] Z. Galazka. Journal of Applied Physics, 131(3), 031103, 2022.
- [3] Chaman, et al. Japanese Journal of Applied Physics, 61(5), 055501, 2022.
- [4] Li, Wenshen, et al. IEEE Electron Device Letters 41.1 (2019): 107-110.

A capacitance-coupled Ga2O3 memristor

Dr Yaonan Hou^{1,2}, Prof. Lijie Li^{1,2}, Prof Zengxia Mei^{3,4}, Dr Huili Liang^{3,4}, Mr Alfred Moore¹

¹Electronic and electrical engineering, Swansea University, , ²Centre for Integrative Semiconductor Materials (CISM), Swansea University, ³Songshan Lake Materials Laboratory, ⁴Institute of Physics, Chinese Academy of Sciences

A memristor is a nonlinear resistance switching device, regarded as a promising electronic component for neuromorphic computing as a scheme for realising artificial intelligence (AI). There is substantial progress in realising memristors using binary oxide materials including but not limited to TiOx, ZnOx, ZrOx etc. [1-3] Among these, Ga2O3 is an emerging semiconductor with unique properties, such as the large bandgap of 4.9 eV and chemical stability. Compared with the six single crystal phases (i.e. α , β , γ , δ , ϵ , κ), amorphous (a) Ga2O3 shows good electrical and optical properties with low-cost deposition approaches, opening a way for large-area manufacturing. The recent advances in a-Ga2O3 memristors focus on increasing the on-off ratio whilst the working scheme is still unclear.

In this work, we have developed a capacitance-coupled memristor (C-Memristor) on a-Ga2O3 film deposited by magnetron-controlled sputtering. Unlike the so-far reported Ga2O3 memristors, our C-Memristor exhibits a polar switching depending on the voltage (current) scan direction, offering easy readout status. Moreover, the frequency measurement shows our device can work in the MHz range. To explain the working mechanism, we have established a model comprising an equivalent circuit together with the oxygen vacancy charge conducting theory. The model well matches our observations. We envisage that the coupled variable capacitance will bring an additional degree of freedom for developing memristor-based synaptic neural circuits in future.

References:

1. D.-H. Kwon, K. M. Kim, J. H. Jang, J. M. Jeon, M. H. Lee, G. H. Kim, X.-S. Li, G.-S. Park, B. Lee, S. Han, M. Kim, and C. S. Hwang, "Atomic structure of conducting nanofilaments in TiO2 resistive switching memory," *Nat. Nanotechnol.* 5, 148–153 (2010).
2. S. S. More, P. A. Patil, K. D. Kadam, H. S. Patil, S. L. Patil, A. V. Pawar, S. S. Kanapally, D. V. Desai, S. M. Bodake, R. K. Kamat, S. Kim, and T. D. Dongale, "Resistive switching and synaptic properties modifications in gallium-doped zinc oxide memristive devices," *Results Phys.* 12, 1946–1955 (2019).
3. H. Yildirim and R. Pachter, "Extrinsic dopant effects on oxygen vacancy formation energies in ZrO2 with implication for memristive device performance," *ACS Appl. Electron. Mater.* 1, 467–477 (2019)

Temperature-dependent investigation of polarisation doping in 330 nm ultraviolet light-emitting diodes

Peter Milner¹, Vitaly Z. Zubialevich¹, Sandeep M. Singh¹, Brian Corbett¹, Peter J. Parbrook¹

¹Tyndall National Institute, ²School of Engineering, University College Cork, ³Centre for Nanoscience and Technology, University of Sheffield

The development of ultraviolet light-emitting diodes (LEDs) has been limited by the poor conductivity of p-(Al)GaN. Polarisation doping has been shown to greatly increase the hole concentration in AlGa_N films. The behaviour of LEDs with polarisation-doping as a function of temperature warrants study owing to the temperature-insensitive carrier concentration, while the benefit of concurrent Mg doping is not clear for this composition range. In this work, three LED structures were grown by metalorganic chemical vapour deposition, with varied p-doping strategies. The structures were nominally the same up to and including the active region. The first LED ('codoped'), consists of a 30 nm Al_{0.35}Ga_{0.65}N electron blocking layer with the final 20 nm Mg-doped. Then a 50 nm graded p-Al_xGa_{1-x}N:Mg layer with $x = 0.35-0.00$ forms the polarisation doped layer. A 'polarisation-doped' LED is compositionally identical to the codoped LED, but no Mg precursor was flowed. A reference LED utilises Mg doping only in p-Al_{0.18}Ga_{0.82}N for p-type conductivity. All LEDs were topped with a 10 nm p-GaN contact layer. Standard fabrication processing was performed to realise 100 μm diameter mesas.

Both LEDs utilising polarisation doping show a steady monotonic increase in QW-related electroluminescence intensity (ELI) from 300 K down to 12 K, with the codoped LED showing the strongest ELI throughout. The reference LED also shows QW emission at 12 K, but has a more complex progression with temperature. A longer wavelength peak associated with Mg-related defects, seen in both Mg-containing LEDs, is completely absent in the polarisation-doped LED. The voltage required for 5 mA in the reference LED increases by 2 V at low temperature, while the polarisation doped LED demonstrates a constant voltage. Better performance from codoping differs from studies investigating higher Al content structures, suggesting the optimum p-type doping conditions for graded AlGa_N is composition dependent.

Gbps UV-C Communications Up To 30 Metres using 235 nm and 255 nm commercial DUV LEDs

Hichem Zimi¹, Doctor Jonathan McKendry¹, Doctor Sina Babadi², Doctor Behnaz Majleseini², Doctor Isaac Osahon², Doctor Johannes Herrnsdorf¹, Professor Harald Haas², Doctor Martin Dawson¹

¹University Of Strathclyde, ²University of Cambridge

Deep ultraviolet (DUV) or UV-C light (210 nm to 280 nm) is attracting significant scientific interest due to its wide range of applications including sterilization, sensing, and curing of materials. UV-C is particularly interesting for optical communications, as it allows communication in a “noise free” channel and can support non-line-of-sight (NLOS) communications thanks to strong scattering of UV light. In addition, UV-C LEDs are witnessing significant improvements in their output powers, efficiencies, and range of available wavelengths [1]. Here we report the demonstration of commercially sourced UV-C LEDs, with peak emission wavelengths of 235 and 255 nm, for optical wireless communications at data rates and distances up to 2 Gb/s and 30 m, respectively.

The current-voltage (I-V), output power, and modulation bandwidth characteristics of the two LEDs were characterized. Maximum optical outputs power achieved are 0.32 and 1.5 mW for the 235 and 255 nm LEDs, respectively, with corresponding turn-on voltages of 5.4 V and 4.7 V. Maximum modulation bandwidths of 60 MHz and 57 MHz for 235 and 255 nm, respectively, were measured using a network analyser.

For line-of-sight optical wireless communications (OWC) the transmitted light was collimated and transmitted over distances up to 30 m to a 1 GHz bandwidth avalanche photodiode. Orthogonal frequency division multiplexing (OFDM) with adaptive bit loading was used to encode data on the LEDs’ output. The maximum “error-free” data rates achieved (Fig 3) , defined here as the highest data rate having a BER lower than 3.8×10^{-3} , were 1.1 and 2 Gb/s for the 235 and 255 nm LEDs, respectively. This work represents, to the best of our knowledge, the first optical wireless links obtained using very short wavelength UV-C at such distances, demonstrating a route towards practical solar blind and non-line-of-sight communications using UV light.

Evaluating Ohmic Contacts to Si-doped Cubic GaN Epilayers

Surender Subburaj^{*1}, Menno J Kappers², Rachel A Oliver², and David J Wallis^{1,2}

¹Centre for High frequency Engineering, Cardiff University, Cardiff, United Kingdom

²Dept. of Materials Science and Metallurgy, University of Cambridge, United Kingdom

Group III-nitrides have the capability to crystallize in two main structures: the stable wurtzite (hexagonal) form and the metastable zincblende (cubic) form. Although hexagonal GaN has traditionally dominated device technologies, there is a resurgence of interest in cubic GaN to address limitations [1]. Cubic III-nitrides lack internal electric fields, potentially enhancing LED efficiency, especially at high drive currents and longer wavelengths [2]. This present study focuses on electrical properties of metal contacts and doping in cubic Si-doped GaN layers grown by Metal Organic Vapour-Phase Epitaxy (MOVPE) on 3C-SiC/Si(001) templates. The transmission line measurements (TLM) method is utilized to assess contact resistance and sheet resistance, crucial for understanding and optimization of device performance [3].

Figures 1a), b) and c) depict the current-voltage (I-V) characteristics of linear-TLM structures on Si-doped cubic-GaN layers (target carrier concentrations (a) $1 \times 10^{17} \text{cm}^{-3}$ (b) $1 \times 10^{18} \text{cm}^{-3}$ and (c) $2 \times 10^{19} \text{cm}^{-3}$). They show linear behaviour across all curves, indicating high quality ohmic contacts. Figure 1d) shows the relationship between contact spacing (d) and resistance (R), with data fitted to a straight line yielding least square fit (R^2) values close to 1, indicating excellent TLM data quality. The tabulated values for the highest Si doped sample are consistent with those observed for high-quality contacts using an identical process to hex GaN n-type layers. Figure 1), (a-c) I-V characteristics measured between pairs of contacts at different distances; (d) extracted resistance plotted versus distance calculated from TLM model. Table: Values of Transfer length, Contact resistance and Sheet resistance as a function of targeted Si doping concentration

Having established high-quality contacts to cubic n-GaN we will use these for development of cubic GaN opto-electronics devices.

Multimodal micro-spectroscopy characterisation of wurtzite InGaN green LEDs

Kimberly Nicholson^{1*}, Raed Alshammary¹, Eve Burgess¹, Chen-Kai Kao², Oleg Laboutin², Hugues Marchand², J. Iwan Davies³, Sara-Jayne Gillgrass¹, Craig Allford¹ and Naresh Gunasekar¹

¹School of Physics and Astronomy, Cardiff University, Cardiff CF24 3AA, UK ;²IQE KC, LLC, 200 John Hancock Road, Taunton, MA 02780, USA; ³IQE plc, Pascal Close, St. Mellons, Cardiff CF3 0LW, UK

InGaN-based LEDs grown on Si have revolutionised room lighting and are gaining tremendous interest for full-colour displays. A key challenge for the epitaxial growth of InGaN-based long-wavelength LEDs (green¹ and red) on Si is strain management. Various strategies for strain management, such as optimising the MQWs, buffer layers, superlattices, electron blocking layers (EBLs), and growing on various crystal orientations, phases, and substrates, are currently being used. These strategies have yielded considerable improvements in quantum efficiency. However, extended defects and residual strains of varying quantities are often observed due to the heteroepitaxial nature of III-nitrides on Si. While their presence impacts device performances, they are not show-stoppers², limiting the commercialisation of the GaN-on-Si platform. An optimised epitaxial wafer fulfilling the required device functionality is of utmost importance in the supply chain, requiring rapid and reliable materials characterisation methods, which is the focus of this work.

Here, we present structural, optical and electrical characterisation results from LEDs targeted for 520 - 570 nm light emission grown in two MOCVD processes (P1 and P2) on 200 mm Si substrates. A representative schematic of wafer A from P1 and wafer B from P2 is shown in Fig.1a and 1c, and their corresponding backscattered electron (BSE) images are shown in Fig. 1b and 1d respectively. Electron channelling contrast imaging (ECCI)³ is used to quantify the threading dislocation densities for all the samples in the order of 10⁸ cm⁻². Raman spectroscopy is used to calculate the stress and strain using GaN E₂(high) phonon mode, where we observe residual tensile strain in wafer B and an additional shoulder peak (see Fig 1e) for wafer A, which has V-pits and micro cracks. Electrical characterisation on the fabricated devices shows wafer B has a lower turn-on voltage and almost twice higher EQE compared to wafer A, demonstrating the importance of optimised InGaN layers⁴ between the MQWs and n-GaN.

References:

1 Usman et al., Critical Reviews in Solid State and Materials Sciences, 46, 450 (2020)

2 Lester et al., Appl. Phys. Lett. 66, 1249 (1995).

3 Naresh-Kumar et al., J. App. Phys. 131, 075303 (2022).

4 Chuanyu Jia et al., Superlattices and Microstructures, 97, 417 (2016).

Applications of energetic ion beams for semiconductor surface modification and characterization at Surrey Ion Beam Centre

Nianhua Peng

Advanced Technology Institute, University of Surrey

The Surrey Ion Beam Centre, as a central part of UK National Ion Beam Centre, is a national research facility supported by UKRI/EPSC. We provide ion beam services for academic researchers and industrial developers based both in UK and overseas. For many years, surface modification and characterization of semiconductor materials have been our major research and service areas. We provide flexible atomic doping with various dopants for different applications, for controlled creation of lattice damage for the fine tuning of carrier mobility, and smart cut of bulk crystal to get high quality thin films etc. Advanced ion beam analysis techniques have also developed for surface layer characterisations using MeV ion beams. These include Rutherford backscattering, particle induced x-ray emission, elastic recoil detection etc. This presentation aims to provide an overview on our capability, in particular for postgraduate students in nitrides research.

Luminescence properties of dislocations in α -Ga₂O₃

M. Maruzane¹, Y. Oshima², O. Makydonska¹, P. Edwards¹, R. Martin¹, F. Massabuau¹

¹University of Strathclyde, Glasgow, UK.

²National Institute for Material Science, Tsukuba, Japan

*E-mail: mugove.maruzane@strath.ac.uk

α -Ga₂O₃ is a meta-stable polymorph of Ga₂O₃ with a corundum structure and a reported band gap of 5.1-5.3 eV, which is the highest amongst the family of polymorphs. Therefore, α -Ga₂O₃ is a promising candidate for applications in high-power electronics and solar-blind photodetectors, moreover, the corundum nature of α -Ga₂O₃ means that it is a more viable option for alloying with other corundum oxides e.g., Al₂O₃, In₂O₃ [1].

Epitaxy lateral overgrowth (ELOG) is a process used to reduce the density of defects in a semiconductor from an estimated 10^{11} cm⁻² to a density of 10^5 cm⁻² [2-3]. The process also presents the benefit of isolating dislocations in the material, allowing studies on the effects of dislocations in semiconductors [3]. The impact of dislocations on the luminescence properties of α -Ga₂O₃ is not fully understood; however, the recent successful deposition of α -Ga₂O₃ ELOG samples can help us build an understanding of this defect.

Cathodoluminescence is a commonly used technique to characterise the luminescence properties of semiconductor materials with a nanometre scale. In this study, we employ a cathodoluminescence mapping technique to investigate the optical properties of dislocations in an ELOG film of α -Ga₂O₃. The average cathodoluminescence spectrum of α -Ga₂O₃, corrected for system response, had a resultant spectrum consisting of three broad luminescence lines. We observe the first line at 3.3-3.4 eV corresponding to self-trapped holes recombination with free electrons [4]. A second line at 3-3.2 eV has been assigned by previous work to donor-acceptor pair recombination involving gallium and oxygen vacancies [4]. Finally, we observe a third line at 2.6-2.8eV which has had little discussion in the literature but is assigned to dopants, complexes, and interstitials.

Mapping highlights strong correlations between these lines and the dislocation location. The 3.5-3.7 eV line strongly weakens at the dislocation position and shows a peak shift in the range of 0.1eV. On the other hand, the 3-3.3 eV line exhibits an intensity increase and an energy peak shift of 0.3eV in the vicinity of the dislocation, which indicates point defect segregation at the dislocation. Meanwhile, the line at 2.6-2.9 eV also strongly correlates with the dislocation position, which we interpret as originating from point defect segregation with an energy peak shift of 0.3 eV.

In conclusion, we have conducted the first nanoscale investigation of the properties of dislocations in α -Ga₂O₃. We report a point defects-related luminescence at the vicinity of the dislocation at an energy of 2.6-2.9 eV. The defect is accompanied by a cloud of point defects surrounding it, increasing luminescence at 3-3.2 eV.

References

- [1] Oshima et al., APL, 121,260501(2022).
- [2] Oshima et al., APL Mater, 7, 022503 (2019).
- [3] Son et al, IUCrJ, 8, 462 (2021).
- [4] Ghadbeigi, JofE Mater, 50, 2990–2998, 2021.

Microanalysis of β -(Al_xGa_{1-x})₂O₃ grown by MOCVD

Mugove Maruzane¹, Arpit Nandi², Sean Douglas¹, Lewis Penman¹, Sai Charan Vanjari², Indra Sanyal², Matthew Smith², Rob Martin¹, Martin Kuball², Fabien Massabuau¹

¹ Department of Physics, SUPA, University of Strathclyde, Glasgow, United Kingdom

² Center for Device Thermography and Reliability, University of Bristol, Bristol, United Kingdom

*E-mail: mugove.maruzane@strath.ac.uk

β -Ga₂O₃ is the most stable polymorph of Ga₂O₃ with a bandgap in the range of 4.7-4.9 eV [1]. Al₂O₃ has been successfully alloyed with β -Ga₂O₃ resulting in β -(Al_xGa_(1-x))₂O₃ which has a bandgap in the range of 4.9-7.1 eV [1]. This wider bandgap has been shown to be advantageous for creating deep UV sensors and power electronic devices with high breakdown voltages [2].

β -(Al_xGa_(1-x))₂O₃ thin films have been grown through epitaxial and deposition methods. It has been reported that challenges arise when increasing the incorporation of Al to levels close to x=40% [3]. These challenges are attributed to phase variations and crystal degradation. In this study, we employ wavelength dispersive x-ray (WDX) quantitative analysis, UV-vis spectrophotometry, atomic force microscopy (AFM) and cathodoluminescence (CL) to analyse the effect of increasing Al incorporation on the properties of β -(Al_xGa_(1-x))₂O₃ (x = 0% to *ca.* 40%) films grown by metal-organic chemical vapour deposition on sapphire.

AFM data show that increasing Al incorporation results in an increase in roughness and SEM images shows the presence of elongated features on the surface of each sample. The bandgap energy was observed to increase with Al fraction, following a quadratic relation between composition and bandgap energy [1]. CL reveals that the luminescence spectra of all the samples are very similar in shape, but exhibit a slight blueshift of the UV band commensurate with the increase in bandgap energy.

In conclusion, we have performed characterisation on the influence of Al incorporation. We report the quadratic relation between the Al incorporation and the bandgap. We also observe a blue shift in the peak of the cathodoluminescence with a reduction in the intensity of the CL with increasing Al incorporation.

References

- [1] Peelaers et al., APL, 112.24, 242101 (2018)
- [2] Zhang et al., APL, 112.17, 173502 (2018).
- [3] Kranert et al., JoAP, 117.12, 125703 (2015).

Defect Characterisation of Nitride Semiconductors for High Power Electronics

Miss Aisha Mariam¹, Dr Martin Frentrup¹, Dr Sidra A Dar¹, Dr Menno J Kappers¹, Dr Matthew D Smith², Professor Rachel A Oliver¹

¹University Of Cambridge, ²University of Bristol

Growth of GaN-on-Si has been exploited as a low-cost solution for light emitting diodes. The same epitaxial system is now being explored for use in vertical devices for power electronics, but there are significant concerns regarding the high dislocation densities found in this type of epitaxy, which are expected to negatively impact the performance of the device. Hence, dislocation density reduction in vertical electronic device structures becomes a key concept.

In this study, we present an initial exploration of structures designed for the fabrication of vertical Schottky diodes, consisting of a Si substrate, an AlN nucleation layer, a graded AlGaN layer for stress management, a 1000 nm undoped GaN sub-drift layer, a 200 nm n-doped layer for back-contacting, a 1100 nm drift layer and a 200 nm highly doped layer, to act as the top contact. A SiNx interlayer is incorporated into the sub-drift layer with the aim of reducing the dislocation density.

For samples without a SiNx interlayer, a 100 s NH₃ pre-dose on the Si surface is sufficient to ensure that the wafer remains in convex bow after growth. However, when a SiNx interlayer is incorporated, use of this short NH₃ pre-dose leads to concave bow and cracking. To maintain the strain management after the pre-dose, a longer (190 s) pre-dose is required. Comparison of the x-ray diffraction peak broadening for samples with a SiNx interlayer and with the short pre-dose reveals, disappointingly, a larger peak width for the sample incorporating the interlayer. However, for samples with a longer pre-dose, a thicker SiNx interlayer does lead to a reduced peak broadening relative to a thinner one.

Together these results suggest that controlling dislocation density in GaN-on-Si epitaxy involves a complex interplay of the NH₃ pre-dose with the dislocation reduction structures, which will be explored further in future.

Electrochemical Etching of GaN: Insights into the Role of Etchant pH and Oxalate Anions

Dr Thom Harris-Lee¹, Dr Menno Kappers¹, Prof. Rachel Oliver¹

¹University of Cambridge

Recent research has highlighted the significant potential of porous GaN in advancing the performance of LEDs, sensors, and high-power electronics.[1] An electrochemical etching (ECE) process on doped GaN creates high surface area structures with tunable porosity; thereby improving light extraction and thermal dissipation, and aiding in strain relaxation and defect reduction. However, understanding of the electrochemical mechanisms driving the etching process remains very limited.

ECE is typically conducted by immersing a GaN thin film into an oxalic acid etchant solution and applying an anodic bias potential relative to a counter electrode. In this setup, neither the applied bias potential nor the pH at the GaN surface is effectively controlled, leading to possible drift during etching. To address this, a pH buffer solution based on the oxalate anion can replace oxalic acid, offering enhanced pH control, particularly in highly porous regions where electrolyte diffusion is restricted. Buffer solutions mitigate local pH fluctuations caused by H⁺ production/consumption in the ECE reaction mechanism by utilising the dynamic equilibrium of weak acid dissociation. This approach ensures consistent etching conditions, improving both scalability and reproducibility.

This study investigates the role of etchant pH in ECE, examining porous structures formed across a range of buffered pH levels. These structures are compared with those produced using equivalent concentrations of oxalic acid or sodium oxalate, the individual components of the oxalate-anion-based buffer solution. While the oxalate anion is suspected to play a major role in the etching mechanism,[2] significant differences in the resulting porous structures from different oxalate anion sources suggests other factors may also be involved (e.g., pH). These findings offer new insights into the interplay between etching parameters and reaction mechanisms, facilitating the rational design of advanced porous GaN architectures tailored for specific next-generation optoelectronic and electronic applications.

References

- 1 P. H. Griffin and R. A. Oliver, J Phys D Appl Phys, 2020, 53, 383002.
- 2 A. Shushanian, D. Iida, Z. Zhuang, Y. Han and K. Ohkawa, RSC Adv, 2022, 12, 4648–4655.

Fabrication and characteristics of Quasi-Vertical GaN-on-Si FinFET

Chengzhi Zhang¹, Martin Kuball¹, Matthew D. Smith¹

¹Center for Device Thermography and Reliability, University of Bristol

Gallium nitride (GaN) is a wide bandgap semiconductor material with strong potential in power electronics, with lateral GaN transistors becoming established as the dominant technology in certain high frequency, high power applications such as telecom infrastructure and low frequency GaN-based power device now commercially available. Vertical GaN power transistors can offer improved power density, efficiency and off-state blocking capability than lateral devices and are ideally suited for high voltage applications, although are currently confined to expensive and unsustainable native GaN substrates, preventing commercialization [1], [2], [3]. Implementation of vertical GaN transistors on silicon (Si) substrates (GaN-on-Si) will unlock new market opportunities and thus enable reduced carbon emissions due to improvements in efficiency over competing technologies, although challenges associated with material quality in heteroepitaxial structures must be addressed. Vertical GaN finFETs use a metal-oxide-semiconductor (MOS) gate structure to achieve normally-off operation without the requirement for a buried p-GaN layer used in other vertical GaN transistor technologies [4]. The MOS gate enhances gate reliability and minimizes gate leakage, attributed to the dielectric layer, enabling operation at higher gate voltages while reducing power losses. Furthermore, the absence of a p-GaN layer mitigates challenges such as threshold voltage instability and current collapse, improving overall device performance and reliability. In this work we have demonstrated a Quasi-Vertical GaN-on-Si FinFET with a positive threshold voltage and a high ON/OFF drain current ratio of 10^7 . The devices reveal low subthreshold swings (SSs) down to around 93 mV/dec. Device performance is compared to simulation, with the sub-linear scaling of current output with number of parallel devices attributed to insufficient conductivity in a buried n+GaN layer, highlighting limitations with quasi-vertical configurations, and the steps needed to achieve fully vertical devices is explained.

Modelling of acid etching pathways in porous GaN distributed Bragg reflectors

Mr Piotr Sokolinski¹, Mr Ben Thornley¹, Professor Rachel Oliver¹

¹Department of Materials Science and Metallurgy, University of Cambridge

Distributed Bragg Reflectors (DBRs) are a crucial part of high-efficiency optoelectronic devices, particularly in LEDs [1] and laser cavities [2]. We investigate the fabrication of 5-layer GaN/porous GaN DBRs with high refractive contrast using a single-step electrochemical procedure without the need for additional processing, which preserves surface quality for future device overgrowth [3]. Threading dislocations are utilised as pathways through which acid can penetrate to doped layers and etch to leave behind a mesoporous structure [4]. Current literature suggests that each dislocation is active in all layers [5], but recent experimental data suggests that this is not the case. Instead, the acid can move laterally to switch between dislocation 'pipelines' within the doped layers, which we have named 'cascade' behaviour. We have developed a probabilistic model utilising Python arrays to predict the acid etching pathways and to reproduce the cascade behaviour. From this model, we have also generated current-time plots which correlate to experimental chronoamperometry data. Two distinct etching current regimes were observed experimentally with a smooth transition between them. At low voltages, the current decayed exponentially, whereas at high voltages the current-time plot showed decaying oscillations, each corresponding to the porosification of one doped layer. By manipulating the relative probabilities of the etching of the dislocation and the doped layer, we can reproduce this transition in our model with oscillations being achieved when the dislocations etch much slower than the doped layer and exponential decay achieved when the probabilities are approximately equal. Further investigation is required to develop the physical interpretation of these parameters and to develop an empirical relation between the probabilities and the etching voltage.

Elastic properties of wurtzite BN and boron containing III-N alloys: From first principles to semi-empirical models

Aisling Power^{1,2}, Cara-Lena Nies¹, Stefan Schulz^{1,2}

¹Tyndall National Institute, University College Cork, ²School of Physics, University College Cork

III-nitride alloys, (Al,Ga,In)N, are widely used in optoelectronic devices, as their direct band gaps can, in principle, cover wavelengths from deep UV to red. However, for these extreme wavelength regimes, quantum efficiencies are low [1,2]. Though several factors contribute to this, key issues arise from lattice mismatch in III-N alloy heterostructures, which can lead to high defect densities and connected non-radiative recombination centres [1,2]. Recent studies suggest that introducing wurtzite (WZ) boron nitride (BN) into III-N alloys may resolve these issues due to BN's significantly smaller lattice constant. However, insight into structural, electronic and optical properties of these novel alloys is sparse. Theoretical studies play an important role in determining these fundamental properties and predicting the consequences of combining materials with different electronic structures. The state-of-the-art method for atomistic modelling is ab initio density functional theory (DFT). The “standard” implementation of this framework, however, is computationally expensive and only feasible for small scale systems (<500 atoms). To target heterostructures such as quantum wells or to expedite DFT calculations, semi-empirical models, parameterised against DFT, have found widespread application. Here, we introduce such a model, namely a valence force field (VFF). Building on DFT data and similarities between [111] zincblende and WZ, we establish a semi-analytic VFF parameter determination scheme for binary III-N materials. Transitioning to (B,Ga)N alloys of varying B compositions and alloy microstructures, our model predicts structural properties (e.g. alloy bond lengths distribution) in good agreement with our DFT data. Moreover, we show that when using VFF obtained relaxed atomic positions in DFT electronic structure calculations, band gaps deviate <7%. Thus, our model presents an ideal starting point for future large scale electronic structure calculations of e.g. B-containing III-N quantum wells.

[1] Lin et al 2023 J.Phys. Photonics 5 042502

[2] Amano et al 2020 J.Phys.D: Appl.Phys. 53 503001.

Porous GaN Waveguides: Unlocking New Potential for Hazardous Gas Sensing

Mr Sivaloganathan Kumaran^{1,2}, Dr Bogdan Spiridon¹, Dr Simon Fairclough¹, Dr Saptarsi Ghosh^{1,3}, Mr Jiawei Zhang¹, Mr Benjamin Thornley¹, Dr Thom Harrison-Lee¹, Ms. Francesca Adams¹, Professor Rachel Oliver¹

¹Cambridge Centre for Gallium Nitride, University of Cambridge, ²Cavendish Laboratory, University of Cambridge, ³Centre for Integrative Semiconductor Materials, Department of Electronic and Electrical Engineering, Swansea University

Gallium nitride (GaN) and its alloys are at the forefront of research in wide bandgap semiconductors, renowned for their robust thermal stability, radiation hardness, and exceptional optoelectronic properties. This poster presents a novel application of GaN-based materials: porous GaN waveguides for hazardous gas sensing in critical environments such as nuclear facilities and outer space.

Our research explores simulation, design, and experimental validation to develop porous GaN optical waveguides optimised for mid-infrared absorption spectroscopy. This technique leverages GaN's intrinsic properties enhanced by a porous architecture to maximise evanescent field interaction with target gases. Unlike traditional platforms like silicon-on-insulator or lithium niobate, porous GaN provides tuneable porosity and a higher sensitivity by bringing gas analytes closer to the waveguide's high-field regions. Moreover, its optical transparency in the spectral region of interest lends itself to the detection of different gases, such as carbon monoxide and methane.

We evaluate multiple waveguide configurations, including slab, rib, and ridge geometries, to identify designs that optimise light confinement and sensing performance. Simulation results demonstrate enhanced sensitivity, while experimental validation using techniques such as atomic force microscopy and infrared spectroscopy confirms the viability of these designs.

This research highlights the versatility of GaN as a platform for innovation, bridging fundamental semiconductor physics with practical applications. It paves the way for next generation sensing technologies tailored to thrive in the most demanding and hazardous conditions. The implications of this work extend to other applications requiring robust and selective detection technologies, such as biomolecule, volatile organic compound, and radiation sensing, as well as for operation in other parts of the electromagnetic spectrum. The integration of porous GaN waveguides into real-world devices offers transformative potential for monitoring critical environments and advancing wide bandgap semiconductor research.

Keywords: Gallium Nitride, Porous Waveguides, Hazardous Gas Sensing, Wide Bandgap Semiconductors, Mid-Infrared Absorption Spectroscopy.

COMSOL Multiphysics Modelling of porous gallium nitride distributed Bragg reflectors

Mr. Zetai Xu¹, Mr. Ben Thornley¹, Mr. Sivaloganathan Kumaran¹, Prof. Rachel Oliver¹

¹University Of Cambridge

Previous computational studies on porous distributed Bragg reflectors (DBR) have used the Transfer Matrix Method to compute the DBR reflectance, treating the porous layer as having a uniform effective refractive index, approximated from the geometric mean of GaN and air.

The finite element method allows for more realistic modelling of pore morphologies, by dividing the DBRs into small discrete sections and calculating solutions to Maxwell equations at each section boundary. We selected COMSOL Multiphysics to model a DBR composed of porous and non-porous GaN layers.

The model was first set up as a 2D unit cell, with periodic Floquet boundary conditions on either side; this means that the solution on one side of the unit cell is equal to that of the other side, multiplied by a phase factor. The unit cell was capped with periodic port conditions, one acting as an emitter and listening port at the top of the unit cell, and one at the bottom acting as a listener for any transmitted waves. This allows for perfect transmission of the electromagnetic waves through the port without non-physical reflections. Assuming that the density of pores in a porous GaN layer is consistent throughout, and the porosity of each layer is the same, different pore morphologies were tested.

However, 2D models unrealistically assume that the pores are tubes when extruded from cross-section. Therefore, it was desirable to develop a 3D model that simulates light reflectance from realistic pore morphologies comparable with scanning electron microscopy. Simple conical pores and more realistic star-shaped pores were simulated and compared alongside experimental measurements of DBR pore structures. Results suggest that the model does not yet express fully the microstructure of the material and/or the physics controlling reflectance.

Applications of GaN HEMTs in Cryogenic Power Electronics

Dr. Matthew Pearce¹, Mr. Charley Shi, Mr. Aaron Wadsworth, Miss Francesca Adams, Dr. Rachel Oliver, Dr. Duleepa Thrimawithana, Dr. Rod Badcock

¹The University Of Auckland

Reliable electronics and power electronics operating at extremely low temperatures (below -150°C), known as cryoelectronics, are essential for applications such as aviation, space exploration, nuclear fusion, and particle accelerators. Power electronics is a vital part of any electronics system used to convert input power to a form that is usable by the components (e.g. motors) that require it. Cryogenic power electronics has been shown to exhibit higher performance than their room temperature equivalents, by the means of more efficient and faster switching power switching devices [1]. This makes cryogenic power electronics particularly pertinent to applications with readily available cryogenic cooling such as liquid hydrogen fueled electric aircraft and spacecraft. To date, GaN HEMTs, specifically those with Schottky p-GaN gates, have been regarded as the best power switch for cryogenic power electronics due to its improved characteristics at cryogenic temperatures [2, 3]. This abstract discusses the work to date on cryogenic GaN-based power electronics to date by the team at The University of Auckland, New Zealand.

The team has successfully developed a cryogenic GaN HEMT-based power converter with record-breaking end-to-end efficiency and power density [4]. This required identifying and characterizing off-the-shelf components capable of functioning in cryogenic environments [5, 6]. Novel techniques were devised, particularly for miniaturizing magnetic components [4, 7]. The Auckland team is progressing on integrating features such as isolation, protection, ancillary services, and digital control into the cryogenic environment.

Though the static on-resistance $R_{ds(on)}$ of GaN HEMTs has been extensively investigated and shown to be reduced by almost an order of magnitude at cryogenic temperatures (CT) compared to room temperature (RT) [2,3], their dynamic $R_{ds(on)}$ has not been investigated much at CT. Dynamic $R_{ds(on)}$ is due to charge trapping that modifies the 2DEG charge carrier density and gate threshold voltage, and depends on the device stress voltage, device current, gate source voltage, stress time and temperature [8]. A circuit has been developed to further investigate the phenomenon at CT [9]. Preliminary results have been obtained at RT, and CT results will be obtained shortly.

The practicality of the cryogenic GaN HEMT power stage operating at 77 K was demonstrated by driving a superconducting homopolar motor [10]. The power handling capability of 3 kW has also been demonstrated [4]. The team is exploring future directions including higher power levels, tighter integration, additional applications and reliability investigations.

References:

- [1] H. Gui et al., "Review of Power Electronics Components at Cryogenic Temperatures," IEEE Trans Power Electron, vol. 35, no. 5, pp. 5144–5156, May 2020, doi: 10.1109/tpel.2019.2944781.
- [2] A. Wadsworth, D. J. Thrimawithana, L. Zhao, M. Neuburger, R. A. Oliver, and D. J. Wallis, "GaN-based cryogenic temperature power electronics for superconducting motors in cryo-electric aircraft," Supercond. Sci. Technol., vol. 36, no. 9, p. 094002, Jul. 2023, doi: 10.1088/1361-6668/ace5e7.
- [3] Y. Wei, M. M. Hossain, and H. A. Mantooth, "Comparisons and Evaluations of Silicon and Wide Band Gap Devices at Cryogenic Temperature," IEEE Transactions on Industry Applications, pp. 1–13, 2022, doi: 10.1109/TIA.2022.3225370.

- [4] A. Wadsworth, M. G. S. Pearce and D. J. Thrimawithana, "A Cryogenic 3-kW GaN E-HEMT Synchronous Buck Converter," in IEEE Transactions on Industrial Electronics, vol. 71, no. 7, pp. 7075-7084, July 2024, doi: 10.1109/TIE.2023.3306416.
- [5] A. Wadsworth et al., "Evaluating Common Electronic Components and GaN HEMTs Under Cryogenic Conditions," in 2021 IEEE Southern Power Electronics Conference (SPEC), Dec. 2021, pp. 1–6. doi: 10.1109/SPEC52827.2021.9709441.
- [6] C. Shi et al., "Ancillary Circuitry for a Cryogenic GaN Half-Bridge, " 2024 Southern Power Electronics Conference (SPEC) 2024, Brisbane, Australia, 2024.
- [7] A. Wadsworth, M. G. S. Pearce, D. J. Thrimawithana and L. Zhao, "Dense and Efficient Cryogenic Power Converter Using Stress Annealed and Stacked Nanocrystalline Cores," in IEEE Transactions on Power Electronics, doi: 10.1109/TPEL.2024.3491037.
- [8] G. Zulauf, M. Guacci, and J. W. Kolar, "Dynamic on-Resistance in GaN-on-Si HEMTs: Origins, Dependencies, and Future Characterization Frameworks," IEEE Transactions on Power Electronics, vol. 35, no. 6, pp. 5581–5588, Jun. 2020, doi: 10.1109/TPEL.2019.2955656.
- [9] C. Shi et al., "A Circuit for Evaluating GaN HEMT Dynamic $R_{ds(on)}$ at Cryogenic Temperatures, " 2024 Southern Power Electronics Conference (SPEC) 2024, Brisbane, Australia, 2024.
- [10] F. Gliese et al., "Characterization and Control of a Superconducting Homopolar Motor with Cryogenic GaN Inverter for Electric Aircrafts," 2024 IEEE Energy Conversion Congress and Exposition (ECCE), Phoenix, Arizona, USA, 2024.

Microstructural characterisation of InGaN/GaN MQWs on silicon

Raed Alshammary^{1*}, Kimberly Nicholson¹, Chen-Kai Kao², Oleg Laboutin², Hugues Marchand², Davies³, Naresh Gunasekar¹

J. Iwan

¹School of Physics and Astronomy, Cardiff University, Cardiff CF24 3AA, UK

²IQE KC, LLC, 200 John Hancock Road, Taunton, MA 02780, USA

³IQE plc, Pascal Close, St. Mellons, Cardiff CF3 0LW, UK

*AlshammaryRM@cardiff.ac.uk

InGaN-based blue LEDs have revolutionised the solid-state lighting technologies that underpin the white lighting for our homes and commercial spaces. However, producing full-colour InGaN-based LEDs by heteroepitaxy poses several challenges, the critical one being the lattice mismatch between the substrate and the epilayer and the lattice mismatch between InN and GaN. This mismatch results in a significant compressive strain that restricts indium incorporation. Hence, strain engineering using strain relief layers has become the cornerstone for optimising III-nitride-based devices, as they help create high-quality heterostructures. However, it is still an ongoing task to realise the uniform epitaxial stacks across 200 – 300 mm Si substrates¹.

Herein, we report the structural properties of four InGaN/GaN LED wafers grown using two different MOCVD processes. Samples A (Blue LED) and B (Green LED) were grown using process P1, and sample C (Blue LED) and sample D (Green LED) were grown using process P2. The schematic in the inset of Fig 1a shows typical LED epi-stacks. We employ the structural

characterisation techniques of X-ray diffraction and spectroscopy to assess the stress, and dislocation densities compared Electron diffraction studies. We observed the GaN E_2 (high) phonon mode splitting in samples B. This suggests that the heterostructure is no longer pseudomorphic, suggesting two different types of GaN layers, each distinct stress states². For sample shoulder peak at the lower frequency of A_1 (LO) when excited 532 nm laser (see Fig. 1b) is observed, which can be attributed disorder in the atomic arrangement Indium segregation, also evidenced in the XRD asymmetric (105) scans as shown in Fig. 1d. previous studies on AlGaIn/GaN superlattices show such an A_1 (LO) peaks shifts attributed to zone folding effects³. The absence of such peak splitting in samples C and D, and the lower residual strains measured via Raman and XRD compared to samples A and B, reveal the good structural quality for samples grown using process P2. All the samples show threading dislocation densities of the order of 10^8 cm^{-2} , with sample B showing V-pits and micro-cracks. Our present work demonstrates the importance of rapid and non-destructive characterisation techniques for optimising III-nitrides epitaxy for next-generation light sources.

References:

¹Y. Dai et al., *Appl.Phys. Lett.*, **125**, 2, (2024).

²M. Katsikini et al., *Journal of Applied Physics*, **130**, 20 (2021).

³C. H. Chen et al., *Appl.Phys. Lett.*, **78**, 3035, (2001).

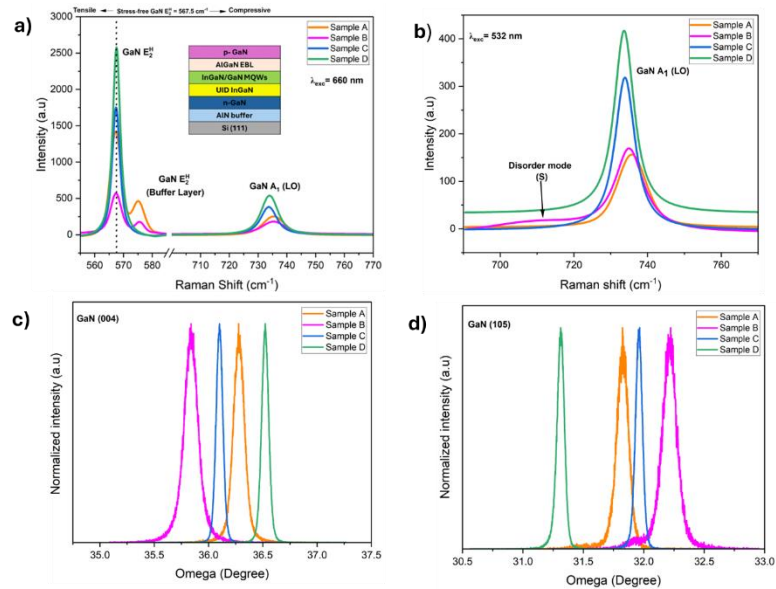


Fig 1. a) Raman spectra of GaN E_2 (high) phonon mode acquired using 660 nm laser excitation and b) A_1 (LO) phonon mode using 532nm laser, c) HRXRD Rocking curve of symmetric (004) and d) asymmetric (105) reflections.

Raman strain, with have A and

with B, a with a to due to